31st Annual International Conference of the IEEE EMBS
Minneapolis, Minnesota, USA, September 2-6, 2009

Statistical Properties of X-Ray Phase-Contrast Tomography

Cheng-Ying Chou and Mark A. Anastasio

Abstract— **Quantitative in-line X-ray phase-contrast tomography methods seek to reconstruct separate images that depict an object's absorption and real-valued refractive index distributions. They hold great promise for biomedical applications due to their ability to distinguish soft tissue structures based on their complex X-ray refractive index values. In this work, we investigate the second-order statistical properties of images in phase-contrast tomography and describe how they are distinct from those associated with conventional absorption-based tomography.**

I. INTRODUCTION

In-line phase-contrast tomography methods [1]–[5] have been developed that produce estimates of the three-dimensional (3D) complex-valued refractive index distribution of an object. Because of its advantages over conventional radiography, X-ray phase-contrast imaging methods [6], [7] are being actively developed for biomedical imaging applications [8]–[10].

Phase-contrast tomography can be interpreted as a two step process. Quantitative in-line phase-contrast imaging methods, operating in planar-mode at a given tomographic view angle, can reconstruct separate images that depict the object's projected absorption and real-valued refractive index distributions, which reflect two distinct and complementary intrinsic object properties. These images can be determined by use of Fourier-based reconstruction formulas [11], [12]. Subsequently, these planar images computed at a collection of view angles are interpreted as tomographic projections from which estimates of the 3D absorption and refractive index distributions are reconstructed.

The statistical properties of conventional X-ray computed tomography (CT) have been systematically explored [13]–[15] in previous studies. However, the reconstructed images in phase-contrast tomography remain largely unexplored. An understanding of the second-order statistical properties of the reconstructed images is important for optimizing system and algorithm designs using task-based measures of image quality [16]. In this work, the covariance of the images reconstructed in phase-contrast tomography are investigated.

II. IMAGING MODEL

We consider the canonical in-line measurement geometry shown in Fig. 1. A rotated Cartesian coordinate system $\vec{r} = (x, y_r, z_r)$ is related to a reference system $\vec{r} = (x, y, z)$ as $y_r = y\cos\theta + z\sin\theta$ and $z_r = z\cos\theta - y\sin\theta$, where θ denotes the tomographic view angle that is measured from the positive y-axis. The axis of tomographic scanning corresponds to the x-axis. A time-harmonic scalar plane-wave U_i with wavelength λ, or wavenumber $k \equiv \frac{2\pi}{\lambda}$, propagates along the positive z_r-axis and irradiates an object. The object is characterized by its complex-valued refractive index distribution $n(\vec{r}) \equiv 1 - \delta(\vec{r}) + j\beta(\vec{r})$, where $\delta(\vec{r})$ and $\beta(\vec{r})$ describe the refractive and absorption properties of the object. The intensity of the transmitted wavefield is recorded on two or more parallel detector planes of constant-z_r, which are spanned by the detector coordinates (x, y_r). Tomographic scanning is performed by simultaneously rotating the plane-wave source and detector about the x-axis. The tomographic view angle θ will be suppressed in the equations below.

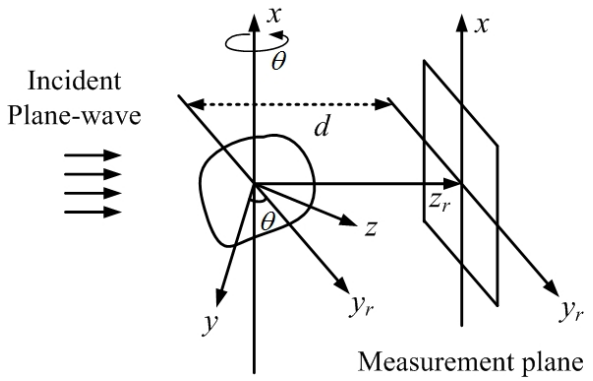

Fig. 1. The measurement geometry of in-line X-ray phase-contrast imaging.

On the contact plane behind the object, the transmitted wavefield is given by

$$U_t(x, y_r, z) = \exp[-A(x, y_r) + j\phi(x, y_r)]U_i, \tag{1}$$

where $A(x, y_r)$ and $\phi(x, y_r)$ define the object's projected X-ray attenuation and refractive, i.e., phase, properties as:

$$A(x, y_r) = k\int dz\, \beta(\vec{r}), \tag{2}$$

and

$$\phi(x, y_r) = -k\int dz\, \delta(\vec{r}). \tag{3}$$

The quantities $A(x, y_r)$ and $\phi(x, y_r)$, computationally determined at a collection of view angles, can be interpreted as the raw projection data corresponding to the 3D quantities $\beta(\vec{r})$ and $\delta(\vec{r})$. To determine $A(x, y_r)$ and $\phi(x, y_r)$ for an arbitrary object, measurements of the transmitted wavefield intensity on two distinct detector planes are generally required. This task is known as phase retrieval.

C.-Y. Chou is with the Department of Bio-Industrial Mechatronics Engineering, National Taiwan University, Taipei, Taiwan chengying@ntu.edu.tw

M. A. Anastasio is with the Department of Biomedical Engineering, Medical Imaging Research Center, Illinois Institute of Technology, Chicago, IL 60616, USA anastasio@iit.edu

III. STATISTICAL PROPERTIES OF RECONSTRUCTED IMAGES

Let $I_m(x,y_r)$ denote the wavefield intensity recorded on the detector plane $z=z_m$, and let $\widetilde{I}_m(u,v_r)$ denote its two-dimensional (2D) Fourier transform with respect to x and y_r. Here (u,v_r) denote the spatial frequency components that are conjugate to the detector coordinates (x,y_r). Similarly, we let $\widetilde{A}(u,v_r)$ and $\widetilde{\phi}(u,v_r)$ denote the 2D Fourier transforms of $A(x,y_r)$ and $\phi(x,y_r)$.

A. Planar images

In near Fresnel zone, the Fourier components of the estimated attenuation and phase functions have second-order statistical properties that behave as

$$\mathrm{Cov}\left[\widetilde{A}(u,v_r,\theta),\widetilde{A}(u',v_r',\theta)\right] \propto \frac{\mathrm{Cov}[\widetilde{I}_s(u,v_r;z_m),\widetilde{I}_s(u',v_r';z_m)]+\mathrm{Cov}[\widetilde{I}_s(u,v_r;z_n),\widetilde{I}_s(u',v_r';z_n)]}{(z_m-z_n)^2}, \tag{4}$$

and

$$\mathrm{Cov}\left[\widetilde{\phi}(u,v_r,\theta),\widetilde{\phi}(u',v_r',\theta)\right] \propto \frac{\mathrm{Cov}[\widetilde{I}_s(u,v_r;z_m),\widetilde{I}_s(u',v_r';z_m)]+\mathrm{Cov}[\widetilde{I}_s(u,v_r;z_n),\widetilde{I}_s(u',v_r';z_n)]}{\lambda^2(z_m-z_n)^2f^2f'^2}, \tag{5}$$

where $\widetilde{I}_s(u,v_r;z_m)$ denotes the Fourier transform of $I_s(x,y_r;z_m)$, $I_s(x,y_r;z_m)=I_m(x,y_r)-1$, $f^2\equiv u^2+v_r^2$, $f'^2\equiv u'^2+v_r'^2$, and $m\neq n$. From knowledge of these second-order statistics, the covariance of the reconstructed tomographic images can be determined as described next.

B. Tomographic images

Estimates of $\beta(x,y,z)$ and $\delta(x,y,z)$ can be determined by use of the parallel-beam filtered backprojection (FBP) algorithm as

$$\beta(\vec{r})=\int_0^\pi d\theta\ \mathscr{F}_2^{-1}\left\{\frac{|v_r|}{D_{m,n}}\left[\sin(\pi\lambda z_m f^2)\widetilde{I}_s(u,v_r;z_m) -\sin(\pi\lambda z_n f^2)\widetilde{I}_s(u,v_r;z_n)\right]\right\}\Big|_{y_r=y\cos\theta+z\sin\theta}, \tag{6}$$

and

$$\delta(\vec{r})=\int_0^\pi d\theta\ \mathscr{F}_2^{-1}\left\{\frac{|v_r|}{D_{m,n}}\left[\cos(\pi\lambda z_n f^2)\widetilde{I}_s(u,v_r;z_m) -\cos(\pi\lambda z_m f^2)\widetilde{I}_s(u,v_r;z_n)\right]\right\}\Big|_{y_r=y\cos\theta+z\sin\theta}, \tag{7}$$

where $\mathscr{F}_2^{-1}\equiv\iint_\infty du dv_r \exp(j2\pi(ux+v_ry_r))$ is the two-dimensional (2D) inverse Fourier transform operator, and $D_{m,n}\equiv 2\sin[\pi\lambda f^2(z_m-z_n)]$.

It can be verified that the covariance of the reconstructed estimate of $\delta(x,y,z)$ can be computed as

$$\begin{aligned}\mathrm{Cov}[\delta(\vec{r}),\delta(\vec{r'})] = &\int_0^\pi d\theta\int_{-\infty}^{\infty}dv_r|v_r|\mathrm{e}^{j2\pi[ux+v_r(y\cos\theta+z\sin\theta)]}\\ &\times\int_{-\infty}^{\infty}dv_r'|v_r'|\mathrm{e}^{-j2\pi[u'x'+v_r'(y'\cos\theta+z'\sin\theta')]}\\ &\times\mathrm{Cov}\left[\widetilde{\phi}(u,v_r,\theta),\widetilde{\phi}(u',v_r',\theta)\right].\end{aligned} \tag{8}$$

A similar expression can be derived for the covariance of the reconstructed estimate of $\beta(x,y,z)$, which involves the quantity $\mathrm{Cov}\left[\widetilde{A}(u,v_r,\theta),\widetilde{A}(u',v_r',\theta)\right]$.

IV. NUMERICAL RESULTS

Computer simulation studies were conducted to investigate the second-order statistical properties of in-line X-ray phase-contrast imaging. A monochromatic X-ray plane-wave with wavelength $\lambda=0.8265\times10^{-10}$ m was assumed to propagate along the positive z_r direction and irradiate an object. A numerical phantom comprised of 2 uniform ellipsoids was employed to represent the object's complex-valued refractive index distribution $n(\vec{r})$. From knowledge of the object, the transmitted wavefield and the subsequent intensity data were determined on two distinct detector planes behind the object. Noisy version of the intensity data were computed by generating realizations of uncorrelated Gaussian random processes with the variance $\sigma^2=10\%$. Tomographic data were formed by repeating the computation at 180 evenly spaced view angles θ over the interval [0,180°).

Subfigures (a) and (b) of Fig. 2 display the covariance estimates of the projected phase and projected absorption images. As predicted in (4) and (5), the pole at zero frequency of the Fourier covariance properties for the phase estimates results in very different covariance properties than that of absorption estimates. The second-order statistical properties of the reconstructed estimates of $\beta(\vec{r})$ and $\delta(\vec{r})$ were computed by use of (8) and are displayed in Fig. 2 (c) and (d). The degree of the noise correlation in the tomographic phase images is reduced, due to the mitigation of the zero-frequency pole by the ramp filter in the parallel-beam FBP algorithm.

V. SUMMARY

In this work, we investigated the statistical properties of the reconstructed images in X-ray phase-contrast tomography. Specifically, we derived analytical expressions for the covariance of the reconstructed 3D absorption $[\beta(\vec{r})]$ and real- valued refractive index $[\delta(\vec{r})]$ distributions. Our

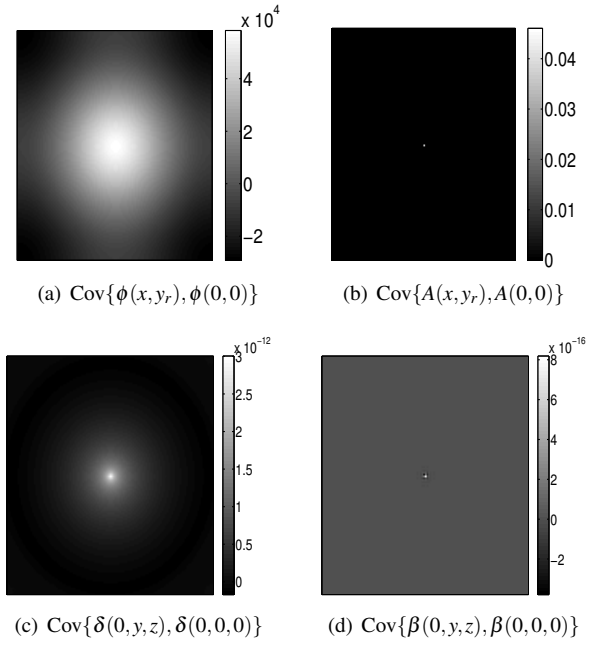

(a) $\mathrm{Cov}\{\phi(x,y_r),\phi(0,0)\}$ (b) $\mathrm{Cov}\{A(x,y_r),A(0,0)\}$

(c) $\mathrm{Cov}\{\delta(0,y,z),\delta(0,0,0)\}$ (d) $\mathrm{Cov}\{\beta(0,y,z),\beta(0,0,0)\}$

Fig. 2. The covariance maps (a) $\mathrm{Cov}\{\phi(x,y_r),\phi(0,0)\}$, (b) $\mathrm{Cov}\{A(x,y_r),A(0,0)\}$, (c) $\mathrm{Cov}\{\delta(0,y,z),\delta(0,0,0)\}$, and (d) $\mathrm{Cov}\{\beta(0,y,z),\beta(0,0,0)\}$

results reveal that the reconstructed estimate of $\delta(\vec{r})$ contains significant image correlations that are not present in the reconstructed estimate of $\beta(\vec{r})$ or a conventional CT image. The effect of these image correlations on signal detectability remains an interesting and important topic for future research.

VI. ACKNOWLEDGMENTS

This work was supported in part by NSF CAREER Award 0546113, and by National Science Council under grant No. NSC 97-2221-E-002-001-MY2

REFERENCES

[1] S. Mayo, T. Davis, T. Gureyev, P. Miller, D. Paganin, A. Pogany, A. Stevenson, and S. Wilkins, "X-ray phase-contrast microscopy and microtomography," *Optics Express*, vol. 11, no. 19, pp. 2289 – 2302, 2003.

[2] A. Barty, K. Nugent, A. Roberts, and D. Paganin, "Quantitative phase tomography," *Optics Communications*, vol. 175, no. 4, pp. 329–336, 2000.

[3] A. V. Bronnikov, "Theory of quantitative phase-contrast computed tomography," *Journal of the Optical Society of America A: Optics and Image Science, and Vision*, vol. 19, no. 3, pp. 472 – 480, 2002.

[4] P. Cloetens, W. Ludwig, E. Boller, L. Helfen, L. Salvo, R. Mache, and M. Schlenker, "Quantitative phase-contrast tomography using coherent synchrotron radiation," in *Developments in X-ray Tomography* III, *Proceedings of the SPIE*, vol. 4503, 2002, pp. 82–91.

[5] P. Spanne, C. Raven, I. Snigireva, and A. Snigirev, "In-line holography and phase-contrast microtomography with high energy x-rays," *Physics in Medicine and Biology*, vol. 44, no. 3, pp. 741–749, 1999.

[6] W. Thomlinson, P. Suortti, and D. Chapman, "Recent advances in synchrotron radiation medical research," *Nuclear Instruments and Methods in Physics Research A*, vol. 543, pp. 288–296, 2005.

[7] R. A. Lewis, "Medical phase contrast x-ray imaging: current status and future prospects," *Physics in Medicine and Biology*, vol. 49, no. 16, pp. 3573–3583, 2004. [Online]. Available: http://stacks.iop.org/0031-9155/49/3573

[8] E. F. Donnelly, R. R. Price, and D. R. Pickens, "Characterization of the phase-contrast radiography edge-enhancement effect in a cabinet x-ray system," *Medical Physics*, vol. 30, pp. 2292–2296, 2003.

[9] S. Fiedler, A. Bravin, J. Keyrilainen, M. Fernandaz, P. Suortti, , W. Thomlinson, , M. Tenhenun, P. Virkkunen, and M. Karjalainen-Lindsberg, "Imaging lobular breast carcinoma: comparision of synchrotron radiation CT-DEI technique with clinical CT, mammography and histology," *Physics in Medicine and Biology*, vol. 49, pp. 1–15, 2004.

[10] F. Arfelli, V. Bonvicini, A. Bravin, G. Cantatore, E. Castelli, L. D. Palma, M. D. Michiel, M. Fabrizioli, R. Longo, R. H. Menk, A. Olivo, S. Pani, D. Pontoni, P. Poropat, M. Prest, A. Rashevsky, M. Ratti, L. Rigon, G. Tromba, A. Vacchi, E. Vallazza, and F. Zanconati, "Mammography with synchrotron radiation: Phase-detection techniques," *Radiology*, vol. 215, pp. 286–293, 2000.

[11] T. E. Gureyev, A. Pogany, D. M. Paganin, and S. W. Wilkins, "Linear algorithms for phase retrieval in the Fresnel region," *Optics Communications*, vol. 231, pp. 53–70, 2004.

[12] D. M. Paganin, T. E. Gureyev, K. M. Pavlov, R. A. Lewis, and M. Kitchen, "Quantitative phase retrieval using coherent imaging systems with linear transfer functions," *Optics Communications*, vol. 234, pp. 87–105, 2004.

[13] K. M. Hanson and D. P. Boyd, "The characteristics of computed tomoraphic reconstruction noise and their effect on detectability," *IEEE Transaction on Nuclear Science*, vol. 25, pp. 160–163, 1978.

[14] R. F. Wagner and D. G. Brown, "Unified SNR analysis of medical imaging systems," *Physics in Medicine and Biology*, vol. 30, no. 6, pp. 489–518, 1985. [Online]. Available: http://stacks.iop.org/0031-9155/30/489

[15] M. F. Kijewski and P. F. Judy, "The noise power spectrum of CT images," *Physics in Medicine and Biology*, vol. 32, pp. 565–575, 1987.

[16] H. Barrett and K. Myers, *Foundations of Image Science*. Wiley Series in Pure and Applied Optics, 2004.